A Quasi-Coherent Electrostatic Mode in ECRH Plasmas on TJ-II*)

Alexander V. MELNIKOV, Leonid G. ELISEEV, Maria A. OCHANDO[1)], Kenichi NAGAOKA[2)], Enrique ASCASIBAR[1)], Alvaro CAPPA[1)], Francisco CASTEJON[1)], Teresa ESTRADA[1)], Carlos HIDALGO[1)], Sergey E. LYSENKO, Jose L. de PABLOS[1)], Maria A. PEDROSA[1)], Satoshi YAMAMOTO[3)], Shinsuke OHSHIMA[3)], HIBP group[1,4)] and TJ-II team[1)]

Institute of Tokamak Physics, NRC "Kurchatov Institute", 123182, Moscow, Russia
[1)]*Laboratorio Nacional de Fusión por Confinamiento Magnético Asociación EURATOM-CIEMAT, 28040, Madrid, Spain*
[2)] *National Institute for Fusion Science, 322-6 Oroshi-cho, Toki 509-5292, Japan*
[3)]*Institute of Advanced Energy, Kyoto University, Kyoto, 611-0011, Japan*
[4)]*Institute of Plasma Physics, NSC KIPT, 310108, Kharkov, Ukraine*

(Received 6 December 2010 / Accepted 16 March 2011)

A new type of instability mode, related to suprathermal electrons, was found in extremely low-density plasmas, (n_e = (0.2-0.5) $\times 10^{19}$ m^{-3}) with electron cyclotron resonance heating and current drive (ECRH/ECCD) in the TJ-II heliac. The quasi-monochromatic density and plasma potential oscillations in the frequency range 20-120 kHz tend to have several "branches" with constant frequency shift between them. The typical amplitude of the mode induced potential oscillations was estimated to be $\Delta\varphi^{EM} \sim 20$ V. The mode branches have an individual and finite radial extent, odd low poloidal structure ($m \leq 5$) and angular phase velocity of poloidal rotation of about 8×10^4 rad/s in the ion diamagnetic drift direction. The contribution of the mode to the turbulent particle flux $\Gamma_{E\times B}$ for the observed wave vectors $k_\theta < 3$ cm^{-1} was found to be small in comparison with the contribution from broadband turbulence.

Keywords: electrostatic eigenmode, suprathermal electron, ECRH, TJ-II.

DOI: 10.1585/pfr.6.2402030

1. Introduction

Instabilities driven by energetic ions have been observed in tokamaks [1, 2] and stellarators [3–7] in regimes with NBI or ICRF heating. The induced modes, Alfvén Eigenmodes (AEs) or Energetic Particle Modes (EPMs) are driven by energy transfer from energetic ions to the waves. Instabilities driven by energetic electrons have been observed in tokamak and helical plasmas [8–11] in regimes with second harmonic ECR heating and current drive. The paper reports on the experimental evidence for a new energetic electron related instability associated with ECRH/ECCD found in low-density plasmas ($n_e < 0.5 \times 10^{19}$ m^{-3}) in TJ-II and will describe the unique characteristic features of this mode.

2. Experimental Set-up

TJ-II is a four-period flexible heliac with low magnetic shear, $B_0 = 1$ T, $<R> = 1.5$ m, $<a> = 0.22$ m and almost shearless magnetic configurations. The rotational transform (the inverse of the safety factor $1/q = \iota/2\pi$) changes from $\iota/2\pi(0) = 1.55$ to $\iota/2\pi(a) = 1.65$ for the standard configuration denoted 100_44_64, and from 1.51 to 1.61 for configuration 100_40_63, where numbers refer to currents in the magnetic field coils. The discussed hydrogen plasmas are formed and heated using two gyrotrons, operated in second-harmonic X-mode at 53.2 GHz with $P_{ECRH1,2} \leq 0.3$ MW each. Low-density ECRH plasmas are characterized by peaked T_e profile with $T_e(0) \sim$700-1000 eV and flat T_i profile, $T_i(0) \sim$70-80 eV. The density profile is hollow, having the maximum around $\rho \sim 0.5$, with a low negative gradient inside for $\rho < 0.5$ and a sharp positive slope for $\rho > 0.5$. Notwithstanding this, the electron pressure profile is peaked due to the T_e profile shape. An important consequence of ECR heating in low-density plasmas is the generation of suprathermal electrons with high perpendicular velocities ($T_{e\perp} \gg T_{e\parallel}$), whose energies increase as density decreases. For densities around 0.5×10^{19} m^{-3}, the mean energy of the suprathermal electron tail is 3-4 times higher than T_e [12], and below that density, fast electron populations with 40-90 keV have been detected [13].

The plasma potential φ is measured directly by the 150 keV Cs^+ Heavy Ion Beam Probe (HIBP) [14, 15], with high temporal (1 μs) and spatial (1 cm) resolution in the radial range $-1 < \rho < 1$, $\rho = r/a$. In these low-density plasmas, the probing beam attenuation becomes negligible, so the beam current I_t represents the local plasma density in the sample volume n_e^{SV} in arbitrary units. The density profile was obtained by calibrating $I_t(\rho)$ versus the interfer-

author's e-mail: melnik@nfi.kiae.ru

*) This article is based on the presentation at the 20th International Toki Conference (ITC20).

ometer central chord. Two HIBP sample volumes are adjusted to be separated poloidally on a given magnetic surface in order to find the poloidal component of the electric field E_{pol} by the difference in the local potential, $E_{pol} = (\varphi_1 - \varphi_2)/\Delta x$, $\Delta x = \rho\Delta\theta \sim 1$ cm [6], limiting the observed k_θ values to maximum 3 cm^{-1}. In this way we measure the radial turbulent particle flux $\Gamma_r(t) = \tilde{n}_e\tilde{V}_r = 1/B_t\tilde{n}_e(t)\tilde{E}_{pol}(t) = \Gamma_{E\times B}$. Simultaneous poloidally resolved I_t measurements provide sufficient data to extract the poloidal mode number m and the phase rotation velocity by cross-phasing two separated signals.

Bolometers provide data of the plasma emission in the range 2 eV to 4 keV. The bolometry system consists of three 20-channel pinhole cameras monitoring the same poloidal section plus three 16-channel cameras at equivalent poloidal positions [16]. A reflectometer provides the outer gradient part of the electron density profile, while a 16-channel heterodyne ECE system provides the T_e profile, when the plasma optical thickness is sufficient. Langmuir probes (LP) measure the plasma (floating) potential and density (ion saturation current) at the edge, while a Mirnov probe (MP) array provides the MHD oscillation measurements.

3. Experimental Results

3.1 Mode observation

In plasmas with strong off-axis ECRH ($\rho_{ECRH} = 0.64$) and on-axis ECRH/ECCD (both co- and balanced), with various values for the driven current $I_{EC} < 2.5$ kA, specific oscillations were found. The observed oscillations seem to be due to the presence of two types of quasi-coherent modes: centrally and peripherally localized. The central mode, having higher frequencies, is detectable by HIBP, Bolometry and ECE signals. The peripheral mode is also visible in LP and MP signals.

This paper reports the features of the central mode, which can be summarized as follows:

1) The frequency spectrum of the mode shows several strikingly pronounced peaks (typically three) - monochromatic oscillations of HIBP I_t in the range of f = 20-80 kHz with a frequency difference $\Delta f \sim 15$ kHz. A typical mode spectrum shows peaks at $f \sim 30$, 45 and 60 kHz as shown in Figure 1 (a-c).

2) Some of the peaks are also detected in HIBP potential, ECE and bolometer signals (but bolometer and ECE signals are limited to 50 kHz); so far these peaks have not been detected in the HIBP toroidal beam shift, which reflects B_{pol} [17].

3) The radial location of the mode, $\rho < 0.6$, is the region of the positive density gradient. Each frequency peak corresponds to its own radial extent, representing the zonal structure. The higher frequency branch, e.g. 60 kHz, is located at the highest local density, $\rho = 0.57$. The lower frequency peaks are localized more inside at lower local densities.

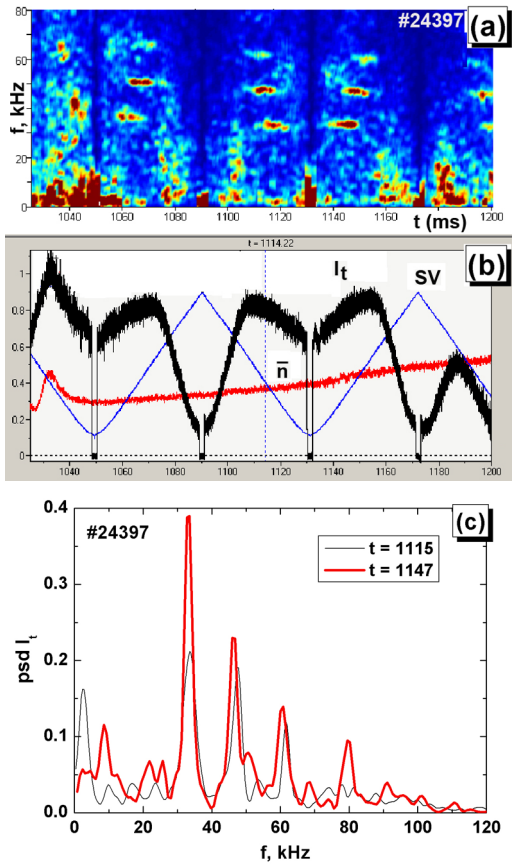

Fig. 1 An example of instability related to suprathermal electrons in the standard magnetic configuration. $P_{ECRH/ECCD}$ = 540 kW, on-axis, refractive indices $N_{||1} = +0.5$, $N_{||2} = +0.28$, $\bar{n}_e = (0.3\text{-}0.5)\times 10^{19}$ m^{-3}; (a) The time evolution of HIBP I_t Power Spectral Density (PSD), representing the plasma density oscillations; (b) the line-averaged density from interferometer (red) in 10^{19} m^{-3}, HIBP Sample Volume (SV) radial positions (blue) and current I_t proportional to density in SV (black) in arb. units; (c) two examples of PSD I_t; location of branches is shown in Table 1.

Table 1 Mode phase characteristics for the example presented in Figures 1 and 4.

f kHz	ρ	k_θ^n cm^{-1}	Ω_θ^{phase} 10^4 rad/s	L cm	m
33	0.30 ± 0.12	0.4 ± 0.10	7.8 ± 1.3	46	2.9 ± 0.7
47	0.41 ± 0.09	0.52 ± 0.10	6.3 ± 1.2	63	5.2 ± 0.8
60	0.49 ± 0.10	0.44 ± 0.10	8.0 ± 1.7	74	5.2 ± 1.3

3.2 Mode characteristics

The mode is quite pronounced in both the plasma potential and density, but not in B_{pol} and magnetic probe signals, so it presents an electrostatic character. The perturbations in the plasma potential and density signals are in antiphase, see Figure 2. The estimations give $\tilde{n}/n \sim k_B e\tilde{\varphi}/T_e$, so the Boltzmann relationship is fulfilled for the mode with $k_B \sim 1$, indicative for the drift-wave instabilities [18]. ECE modulation experiment shows that the mode amplitude de-

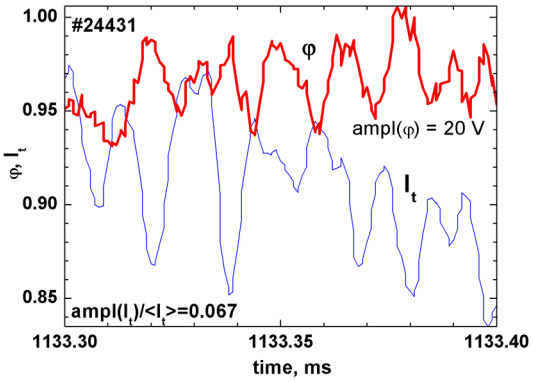

Fig. 2 Potential and density time traces measured by HIBP. Configuration 100_40_63, $\iota/2\pi(a) = 1.6$. $P_{\mathrm{ECRH/ECCD}} = 540\,\mathrm{kW}$, on-axis, $N_{\|1} = N_{\|2} = +0.28$. The mode frequency $f \sim 50\,\mathrm{kHz}$, SV location $\rho = +0.3$, the amplitude in density is $\tilde{n}/n \sim 7\%$, in the potential $\Delta\varphi \sim 20\,\mathrm{V}$. No detectable activity in B_{pol}, so the mode shows "electrostatic" nature.

creases, if $P_{\mathrm{ECRH/ECCD}}$ is lowered, suggesting the importance of the EC power density for the mode excitation (see Figure 3). Although no SXR spectra are available for this particular shot, in previous ECRH modulation experiments [19], it was found that the mean energy of the electron suprathermal tail increases in the phase with the injected EC power. In the discharges discussed here, the mode frequency increases with heating power density, as shown in Fig. 3.

The mode presents a strong correlation between plasma potential and density obtained from two poloidally separated HIBP channels. This observation allows us to retrieve the poloidal wave vector and mode number m:

$$k_\theta = \theta_{n1\,n2}/\Delta x \quad m = Lk_\theta/2\pi, \tag{1}$$

where $\theta_{n1\,n2}$ is a cross-phase between the densities, measured in two sample volumes; L is the length of the poloidal cross-section of the magnetic flux surface [20]. The linear $V^{\mathrm{phase}}_{\mathrm{E\times B}}$ and angular $\Omega^{\mathrm{phase}}_{\mathrm{E\times B}}$ poloidal phase velocities of the mode branch with frequency f are given by

$$V^{\mathrm{phase}}_{\mathrm{E\times B}} = 2\pi f/k_\theta, \quad \Omega^{\mathrm{phase}}_{\mathrm{E\times B}} = V^{\mathrm{phase}}_{\mathrm{E\times B}}/r \tag{2}$$

For the example presented in Figure 1, the mode phase characteristics are shown in Table 1. The potential and density presents the same poloidal cross-phase in the range of $\theta_{\varphi 1\,\varphi 2} = \theta_{\mathrm{n1\,n2}} \sim (0.40\text{-}0.55) \pm 0.10$ rad for all three frequency peaks.

Taking into account the estimated error bars, it can be concluded that all three observed mode frequency peaks are separated in space and rotate with the same angular velocity. The positive sign of k_θ and $V^{\mathrm{phase}}_{\mathrm{E\times B}}$ implies propagation in the ion diamagnetic drift direction.

The mode does not contribute to the turbulent particle flux $\Gamma_{\mathrm{r}}(t)$. Figure 4 shows that unless all the mode frequency peaks are pronounced in both density and E_{pol}

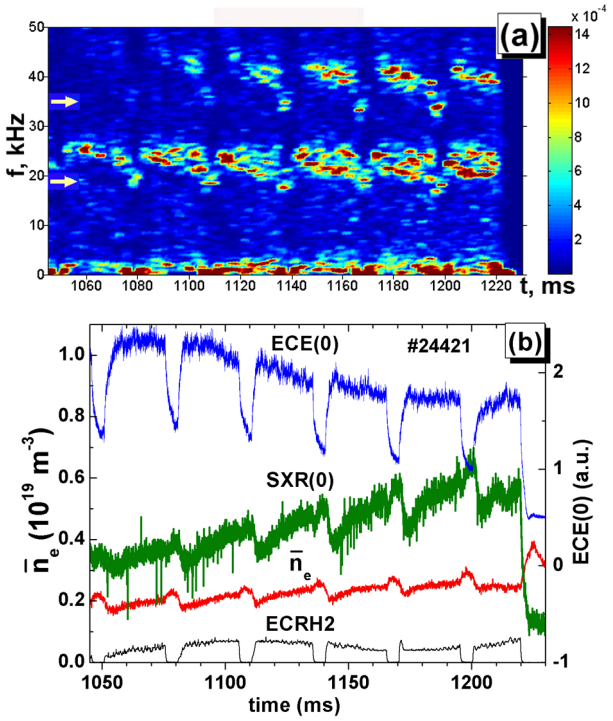

Fig. 3 Mode evolution during on-axis $P_{\mathrm{ECRH/ECCD}}$ modulation. Standard magnetic configuration. $P_{\mathrm{ECRH/ECCD2}} = 250\,\mathrm{kW}$ with 100% modulation, $P_{\mathrm{ECRH/ECCD1}} = 280\,\mathrm{kW} = \mathrm{const}$, $N_{\|1} = N_{\|2} = +0.28$, $\bar{n}_{\mathrm{e}} = (0.18\text{-}0.3) \times 10^{19}\,\mathrm{m}^{-3}$; (a) PSD time evolution of bolometry signal at $\rho = 0.5$. Two mode frequency peaks at $f = 25$ and $40\,\mathrm{kHz}$ are pronounced; lower frequencies (marked by arrows) correspond to lower $P_{\mathrm{ECRH/ECCD}}$. (b) time traces of plasma parameters: SXR(0), ECE(0), representing radiative T_{e} and the central chord line-averaged density $\bar{n}_{\mathrm{e}}$.

spectrograms, they are invisible in the frequency resolved particle flux [21] due to cross-phase $\theta_{\mathrm{Epol\,n}} \sim -\pi/2$, which is valid for all branches [22].

4. Discussion and Summary

In TJ-II, similar to Compass [8], HSX [9], CHS [10], and DIII-D [11], suprathermal electrons related eigenmode (EM) is observed in low-density discharges heated with second harmonic ECRH/ECCD. This EM differs in various features (radial location, mode structure, absence of magnetic component) from other types of quasicoherent modes, earlier found in TJ-II [6, 7, 23–25] in higher density plasmas, or from energetic particle modes found in other machines [8–11]. The EM also differs from GAMs [26, 27], which have different features. More in particular, the EM fulfills the Boltzmann relationship with $k_{\mathrm{B}} \sim 1$, unless have same frequency range. We conclude the EM appears to be a new type of instability, presenting the following features:

1) The EM excited in low-density off-axis ECRH or on-axis ECRH/ECCD plasmas in TJ-II, characterized by suprathermal electron tails. The EM tends to appear as a set of frequency peaks (typically three at 33,

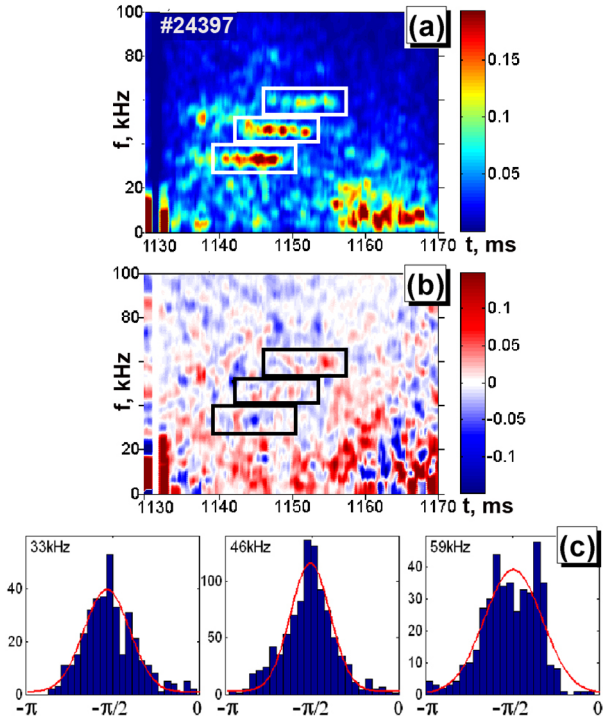

Fig. 4 (a) Time evolution of plasma density PSD, obtained by HIBP radial scan, from $\rho = 0.2$ at $t = 1130$ ms to $\rho = 0.8$ at $t = 1170$ ms, actually represents the radial distribution of the mode. Three quasi-monochromatic frequency peaks are clearly pronounced and a hint of a fourth weaker peak at $f \sim 80$ kHz is seen. (b) Radial distribution of the frequency resolved turbulent particle flux $\Gamma_{E\times B}(f)$. Red color means outward flux, blue – inward flux. The modes are invisible in the spectrogram, so the mode contribution in the total turbulent flux is negligibly small compared to the broadband oscillations. (c) The histograms of the $E_{pol} - n_e$ cross-phase for each marked branches. All three branches present equal cross-phase $-\pi/2$, corresponding to zero flux.

48 and 60 kHz) with constant frequency difference $\Delta f =$ 13-15 kHz. The EM frequency increases with increasing ECRH power.

2) The mode is located in $\rho < 0.6$. According to previous findings, the suprathermal electron population can be confined in the bulk plasma [28]. The mode has a zonal structure: the various frequency peaks of the mode correspond to individual radial areas and have a finite radial extent of a few cm, $\Delta\rho \sim 0.2$.

3) The mode has an electrostatic nature, its potential and density perturbations fulfill the Boltzmann relationship.

4) The mode frequency peaks have odd low ($m \leq 5$) structure and equal angular phase velocities of poloidal rotation in a range of 8×10^4 rad/s into the ion diamagnetic drift direction.

5) The mode contribution to the turbulent particle flux is lower than that of broadband turbulence of the same frequency interval.

Acknowledgment

Russian team was supported by RFBR grants 10-02-01385 and 11-02-00667.

[1] W. W. Heidbrink *et al.*, Phys. Plasmas **15**, 055501 (2008).
[2] S. E. Sharapov *et al.*, Phys. Rev. Lett. **93**, 165001 (2004).
[3] K. Toi *et al.*, Nucl. Fusion **40**, 1349 (2000).
[4] T. Ido *et al.*, Rev. Sci. Instrum. **79**, 10F318 (2008).
[5] A. Weller *et al.*, Phys. Plasmas **8**, 931 (2001).
[6] A. V. Melnikov *et al.*, Nucl. Fusion **50**, 084023 (2010).
[7] A.V. Melnikov *et al.*, Plasma and Fusion Research **5**, S2019 (2010).
[8] M. Valovic *et al.*, Nucl. Fusion **40**, 1569 (2000).
[9] C. B. Deng *et al.*, Phys. Rev. Lett. **103**, 025003 (2009).
[10] M. Isobe *et al.*, Nucl. Fusion **50**, 084007 (2010).
[11] K. L. Wong *et al.*, Phys. Rev. Lett. **85**, 996 (2000).
[12] M. A. Ochando and F. Medina, Plasma Phys. Control. Fusion **45**, 221 (2003).
[13] L. Rodríguez-Rodrigo *et al.*, Proc. 26th EPS Conf. Contr. Fusion and Plasma Phys. (1999) ECA, **23J**, p. 353.
[14] I. Bondarenko *et al.*, Rev. Sci. Instrum. **72**, 583 (2001).
[15] A. V. Melnikov *et al.*, Fusion Sci. Technol. **51**, 31 (2007).
[16] M. A. Ochando *et al.*, Fusion Sci. Technol. **50**, 313 (2006).
[17] Yu. N. Dnestrovskij and A. V. Melnikov, Sov. J. Plasma Phys. **12**, 393 (1986).
[18] P. C. Liewer, Nucl. Fusion **25**, 543 (1985).
[19] F. Medina *et al.*, 31st EPS Conf. on Plasma Physics (London, 2004) ECA, **28G**, P-4.182.
[20] L. G. Eliseev *et al.*, 23th IAEA Fusion Energy Conf. (Daejon, Korea, 2010), EXW/P7-17.
[21] E. J. Powers, Nucl. Fusion **14**, 749 (1974).
[22] A. Melnikov *et al.*, 37th EPS Conf. on Plasma Physics, (Dublin, 2010) P1-066.
[23] L. I. Krupnik *et al.*, 33rd EPS Conf. on Plasma Physics, (Rome, 2006) ECA, **30I**, P-1.138.
[24] L. I. Krupnik *et al.*, AIP Conf. Proc. **875**, 95 (2006).
[25] B. Ph. van Milligen *et al.*, Nucl. Fusion **51**, 013005 (2011).
[26] A. V. Melnikov *et al.*, Plasma Phys. Control. Fusion **48**, S87 (2006).
[27] A. Fujisawa *et al.*, Nucl. Fusion **47**, S718 (2007).
[28] F. Medina *et al.*, Rev. Sci. Instrum. **2**, 471 (2001).